SAN099-1735J

Submit to Nuclear Instruments and Methods in Physics Research B

CORROSION BEHAVIOR OF PLASMA-PASSIVATED Cu

J.C. Barbour, J. W. Braithwaite, K.-A. Son, J. P. Sullivan, N. Missert, and N. R. Sorensen
Sandia National Laboratories, Albuquerque, NM 87185-1056, USA

ABSTRACT

A new approach is being pursued to study corrosion in Cu alloy systems by using combinatorial analysis combined with microscopic experimentation (the Combinatorial Microlab) to determine mechanisms for copper corrosion in air. Corrosion studies are inherently difficult because of complex interactions between materials and environment, forming a multidimensional phase space of corrosion variables. The Combinatorial Microlab was specifically developed to address the mechanism of Cu sulfidation, which is an important reliability issue for electronic components. This approach differs from convention by focusing on microscopic length scales, the relevant scale for corrosion. During accelerated aging, copper is exposed to a variety of corrosive environments containing sulfidizing species that cause corrosion. A matrix experiment was done to determine independent and synergistic effects of initial Cu oxide thickness and point defect density. The CuO_x was controlled by oxidizing Cu in an electron cyclotron resonance (ECR) O_2 plasma, and the point defect density was modified by Cu ion irradiation. The matrix was exposed to 600 ppb H_2S in 65% relative humidity air atmosphere. This combination revealed the importance of oxide quality in passivating Cu and prevention of the sulfidizing reaction. A native oxide and a defect-laden ECR oxide both react at 20°C to form a thick Cu_2S layer after exposure to H_2S, while different thicknesses of as-grown ECR oxide stop the formation of Cu_2S. The species present in the ECR oxide will be compared to that of an air oxide, and the sulfide layer growth rate will be presented.

DISCLAIMER

DISCLAIMER

Portions of this document may be illegible in electronic image products. Images are produced from the best available original document.

INTRODUCTION

This work examines mechanisms critical to corrosion phenomena. Predictive understanding of corrosion is needed to ensure reliability in both electronics and microelectronics components. To date, modeling has been hindered by limited knowledge of primary corrosion mechanisms and the large number of coupled chemical reactions which depend on complex interactions of materials with environment and functionality. This multidimensional problem requires new experimental approaches for quantitative identification of critical phenomena occurring in corrosion phase space. We are examining combinatorial techniques as a first step toward developing these new experimental approaches.

In parallel experimentation, this work varied copper oxide growth and irradiation-induced defect levels to efficiently identify possible mechanisms for copper sulfidation. Atmospheric corrosion of copper was chosen as a typical example of corrosion behavior, and Cu sulfidation is of particular interest to both the electronics and microelectronics industries. This work specifically examined accelerated aging of Cu in a controlled air environment containing H_2S as the sulfidizing agent.

Often, the severity and potential consequence of corrosion are assessed using engineering judgment based on limited historical evidence or accelerated aging experiments after a corrosion problem emerges. The prediction of where the corrosion problem may arise can be accomplished more successfully through sophisticated computer modeling, if the mechanisms on which the models are built have been verified by experimentation. The problem is to understand the corrosion mechanisms and kinetics in order to model the correct corrosion processes, including the ability to predict corrosion events that would be unexpected from existing empirical data. Therefore, a fundamental understanding of the complex phase space of materials, environmental conditions, and component function which causes enhanced or unexpected corrosion rates is required. This paper is the first to examine the use of combinatorial techniques to experimentally determine the corrosion phase space for the important example of atmospheric copper sulfidation.

Predictive, continuum level models for copper sulfidation depend on the development of physically-based atomistic models for surface adsorption, solid-state diffusion, and chemical reaction mechanisms. The literature indicates that in the initial stage of the corrosion process, a layer of "water" adsorbs on the oxide surface, Cu_2O, and sulfur containing reactants interact at the "water" oxide interface. During this stage, solid-state diffusion of Cu through Cu_2O is thought to control the kinetics of Cu_2S island growth on Cu_2O. As the islands coalesce and the Cu_2S layer becomes continuous, solid-state diffusion through Cu_2S begins to control the kinetics of the sulfidation process. A schematic illustration of this sulfidation process is depicted in Fig. 1. However, defining the actual rate-controlling Cu corrosion mechanism(s) and the resultant morphology of the corrosion product has proven to be far more complicated than the literature had initially indicated. Relatively thick sulfide layers were formed with variable morphology in a wide range of environmental conditions, but discontinuous tree-like structures can be formed when these environmental conditions are changed. Presently, a complete set of key mechanisms controlling the corrosion process is not known.

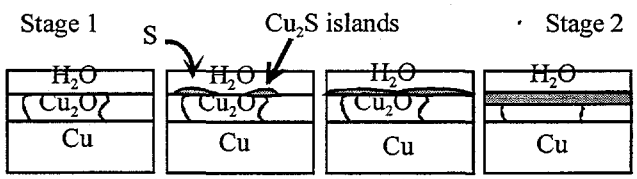

Fig. 1. Illustration of sulfidation process proposed by T. E. Graedel [see, J. Electrochem. Soc. **134**, 1632 (1987)].

Current experimental approaches cannot and do not address the challenging task of identifying the "conditions" leading to enhanced or unexpected aging, because only a small subset of the corrosion

phase space can be examined and the interplay between synergistic factors which could cause corrosion events cannot be identified. Even a reduced set of traditional experiments using a modern design of experiment approach is a daunting task if the entire matrix of environment, materials, and performance factors is included. A more efficient approach is to combine parallel miniature experimentation with ultrasensitive microanalytical techniques to explore this phase space and identify corrosion mechanisms and kinetic parameters in what we have termed the "Combinatorial Microdomain Laboratory" (CML). This paper reports on the initial results from the CML approach and addresses the following questions: 1. How does the nature of the oxide affect the initiation of sulfidation?, and 2. How does the sulfidation reaction proceed?

EXPERIMENT

Our first view of a combinatorial matrix of experiments is shown schematically in Fig. 2. A Cu film is deposited onto a substrate and through the use of shadow masking the film is exposed to various oxidizing environments to change the type and thickness of Cu oxide. In addition, regions of the sample are ion irradiated to different fluence levels in order to vary the point defect concentration in the different oxide layers. In this way, the questions given above could be tested. First, we needed to form a dense copper oxide which was relatively stable to attack by H_2S when compared to the native oxide, and a plasma oxide was chosen to simulate this dense oxide. The density of the native oxide was thought to be low (or the point defect level high) in comparison to the plasma oxide, and therefore the effects of vacancy-mediated sulfidation were simulated by introducing varying levels of point defects in the plasma oxide layer. This matrix of samples is then exposed to a humid air environment containing H_2S as the sulfidizing agent, and the amount of sulfide formed in each cell of the matrix is readily seen and quantitatively measured through ion beam analysis. In this way, ambiguities relating gas flow patterns, humidity levels, and sample reproducibility are minimized by performing the matrix of experiments simultaneously.

For this experiment, Cu films were electron beam evaporated (0.1 nm/s) onto SiO_2 coated Si wafers (chosen as inert substrates) and then exposed in-situ to either a backfill of O_2 gas at 1 Torr pressure and 25°C, or an electron cyclotron resonance (ECR) O_2 plasma at temperatures varying from 35°C to 150°C. The corrosion rate from the deposited Cu was compared to that for "bulk" Cu 101 foils and found to be the same. Different O_2 exposures were meant to simulate a native dry-air-formed oxide for the O_2 backfill, and a more aggressive but controlled oxidizing environment in an O_2 plasma. The O_2 pressure during ECR plasma oxidation was $6x10^{-5}$ Torr. The plasma was composed of O_2 molecules, energetic O atoms, and molecular O_2^+ ions with an energy of approximately 30 eV. The Cu-oxide thickness was increased, as shown in Fig. 2, by exposure to the O_2 plasma for longer periods of time. Vertical strips of sample were then irradiated with 200 keV Cu^+ ions over the fluence range from $1x10^{12}$ Cu/cm^2 to $1x10^{15}$ Cu/cm^2 The range of these ions (see Fig. 3. Below) is ≈58 nm and the straggling is such that doping of Cu in oxide layer is negligible for the 10^{15} cm^{-2} irradiation. The samples were then exposed at 24°C to a humid air atmosphere (65% relative humidity) containing 600 ppb H_2S for up to 72 hrs.

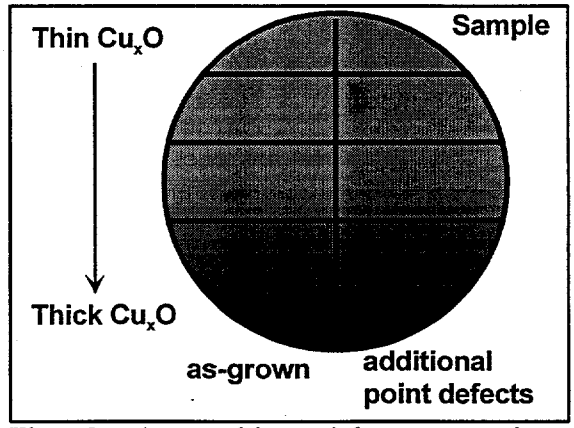

Fig. 2. A combinatorial-type matrix of copper oxide experiments in which the type and thickness of oxide are varied vertically while the level of point defects is varied horizontally.

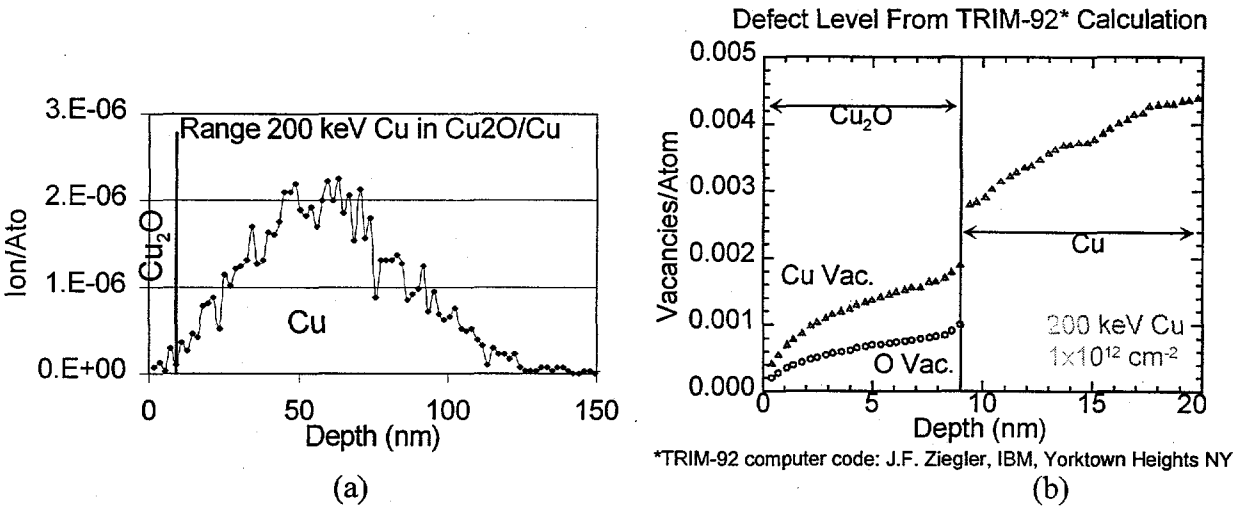

Fig. 3. Ion range (a) and point defect level (b) for 200 keV Cu irradiation of Cu_2O/Cu structure irradiated to a fluence of $1x10^{14}$ Cu/cm^2.

RESULTS

The combinatorial microlab approach to understand H_2S sulfidation of Cu started with a computational derivation of the difference in vacancy migration energies in copper and copper oxide doped with small amounts of In or Al (J. Nelson, private communication). This work was suggested by work on $CuInSe_2$ and $CuInS_2$ solar cell materials in which anti-site defects (In on Cu sites) are thought to tie-up Cu di-vacancies and thereby decrease the Cu mobility yielding an amazing tolerance and stability for highly defected solar cells. Solid-state diffusion of vacancies and di-vacancies in Cu, Cu_2O, CuO, and Cu_2S are thought to be key mechanisms in determining the kinetics of Cu sulfidation in one region of corrosion space. Copper atoms reach the liquid-solid interface through vacancy and di-vacancy diffusion, but the role and energetics of vacancy diffusion has eluded current macroscopic experiments. Therefore, initial focus in this experiment was on understanding the role of defects with combinations of material parameters. By varying the oxide thickness and oxide species in this first sample matrix, we could determine the relative passivation strength of the different types of oxide as well as test the mechanism of solid-state diffusion-controlled growth by measuring the amount of corrosion product formed for different thickness oxides.

The simple optical images shown in Figs. 4 and

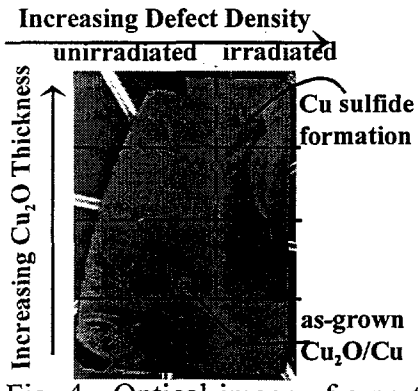

Fig. 4. Optical image of a portion of a combinatorial matrix testing the effect of point defects on Cu_2S formation.

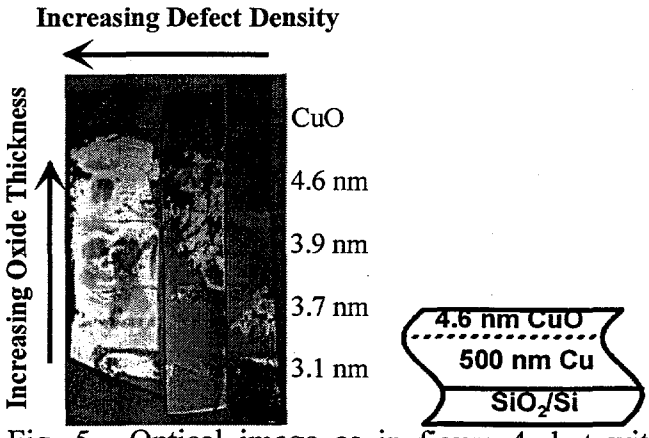

Fig. 5. Optical image as in figure 4, but with lower fluence ion irradiation.

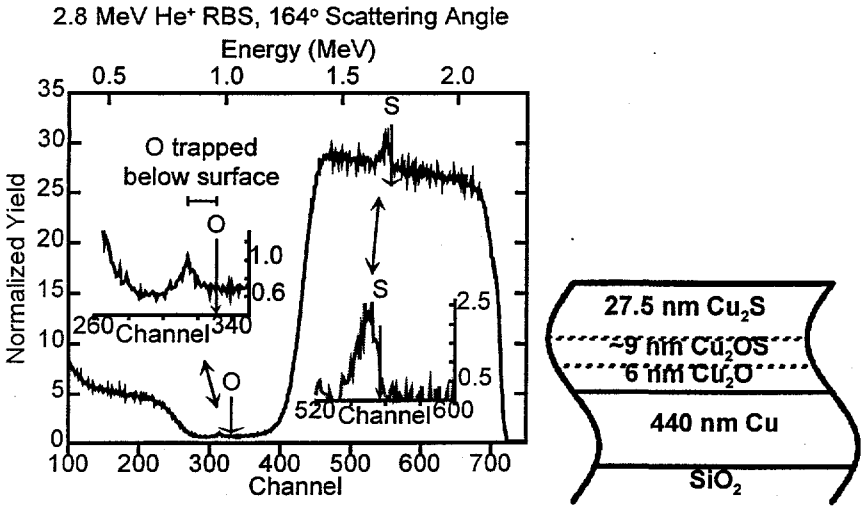

Fig. 6 Rutherford backscattering analysis from one cell of the matrix of experiments shown in fig. 4. This cell was irradiated and treated for 5.5 Hrs in 65% RH, 600 ppb H_2S air at 24°C.

5 demonstrate the important role of the copper oxide and the role played by defects created in a dense plasma-grown oxide irradiated with 200 keV Cu^+ ions. The Cu film was deposited and ECR O_2 plasma oxidized to form 4 different CuO thickness layers as shown. A portion of the sample in fig. 4 (upper right to middle right) was then irradiated to a fluence of $1x10^{15}$ Cu/cm^2 to create point defects in the oxide and Cu layers and exposed to the H_2S environment for 5.5 hours. For this matrix, only the irradiated regions with increased point defect concentrations reacted to form Cu_2S. Similarly, portions of the sample were irradiated to lower fluences to create fewer point defects, as shown in fig. 5. In this figure, the three strips of sample were irradiated to fluences of 10^{14} cm^{-2}, 10^{13} cm^{-2}, and 10^{12} cm^{-2} (from left to right) and again exposed to a 600 ppb H_2S air atmosphere (65% RH) at 24°C for 5.5 hrs. Visibly, the Cu_2S layer formation appears to increase with increasing point defect levels but is relatively independent of the oxide thickness. The air-formed oxide (not shown) exhibited the greatest amount of sulfidation and the unirradiated ECR-grown oxide (shown at left in fig. 4) exhibited no sulfidation. This is a rather simple matrix experiment, but it demonstrates the power of performing nineteen experiments simultaneously to determine that point defects are more important than oxide thickness in determining the kinetics of sulfidation.

Ion beam analysis from each of the different cells in the matrix shown in fig. 4 helped to show how the sulfidation reaction proceeds. Fig. 6 shows the RBS spectrum for the portion of a sample with an initial CuO/Cu_2O thickness of 5-6 nm, which was irradiated with 200 keV Cu^+ ions to a fluence of 10^{15} cm^{-2}, and then treated for 5.5 hrs in a 600 ppb H_2S / 65%RH air environment at 24°C. A representation of the composition depth profile determined for the sample is shown at right in the figure. Approximately the same thickness of sulfide layer, 27-28 nm Cu_2S, was formed for each of the different initial-thickness oxide layers; thereby, confirming the observations deduced from the optical imaging. The Cu_2S grew on top of a layer with mixed oxygen and sulfur content (possibly representative of the porous structure in the top sulfide layer, a ternary compound, or a layer of mixed oxide and sulfide phases). These sulfur containing layers were present on top of a Cu_2O layer (thicker than the initial CuO layer). The existence of this buried oxide layer suggests that either Cu diffuses through the oxide to react and form the sulfide layer causing the oxide layer to become buried, or the oxide layer is sulfided in such a fashion that oxygen is released and caused to diffuse deeper into the substrate where it reacts with Cu to form Cu_2O. While the latter reaction mechanism seems less plausible, marker experiments are required to determine the predominant diffusing species and the interface boundary motion.

The fact that the amount of oxygen in the sample is increasing during the sulfidation process suggests that more complicated coupled reactions are occurring in these initial stages of corrosion than simply explained by the model of Graedel given above. It also suggests that further work is required to

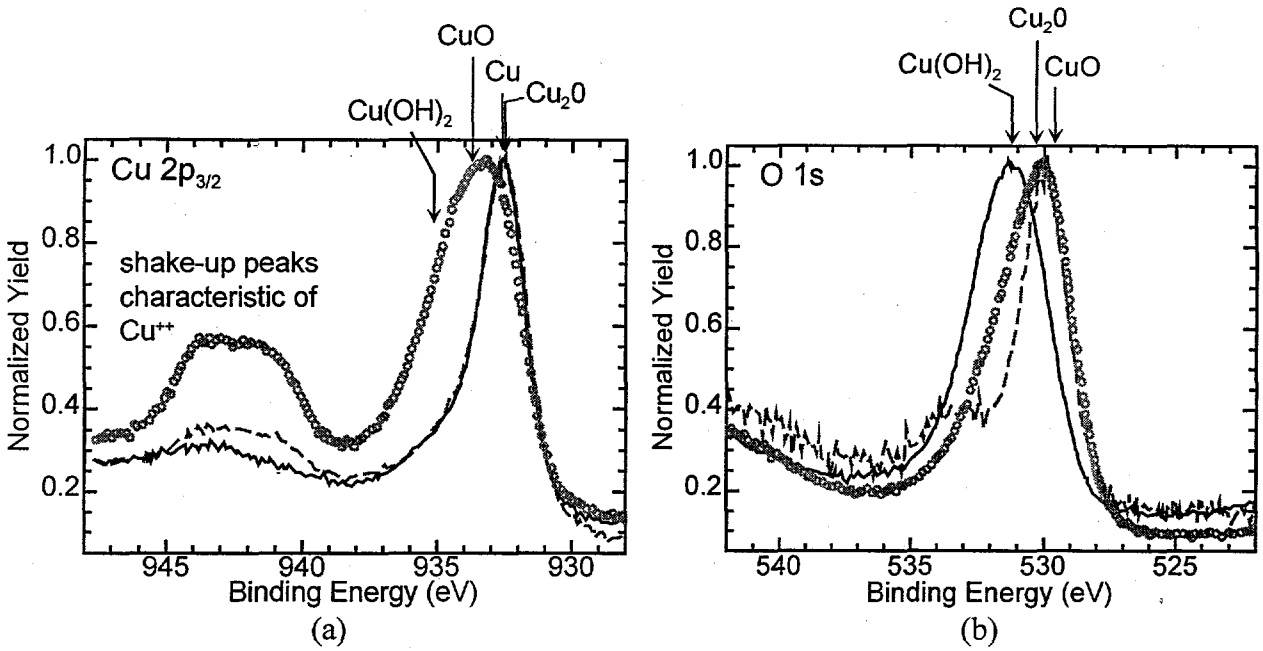

Fig. 7. A comparison of air oxidized Cu and ECR-oxidized Cu $2p_{3/2}$ (a) and O1s (b) XPS signals using Al Kα X-rays. The sample preparation conditions are as follows: light gray circles = 32 nm thick ECR oxidized Cu, dashed line = ~4 nm thick ECR oxidized Cu, solid line = ~1.4 nm thick air oxidized Cu. The Cu $2p_{3/2}$ and O 1s alone are not sufficient to identify Cu vs. Cu_2O vs. CuO. The Cu LMM Auger signal is also required.

understand hydration and oxide grow in the H_2S or other complex air environments. Finally, note that for the air-formed Cu_2O and the CuO layers with a higher level of irradiation ($\geq 10^{14}$ Cu/cm^2), the sulfidation does proceed in a more uniform fashion across the surface of the sample, but for lower irradiation levels the sulfidation process proceeds irregularly across the surface (or not at all for the unirradiated sample).

The behavior of the samples irradiated to different fluence levels can be understood more fully by examining the Cu $2p_{3/2}$ and O1s XPS signals, and the Cu LMM Auger signal. The Cu $2p_{3/2}$ spectrum can show a shakeup peak which is characteristic of Cu(II). In addition, peak shifts from the other signals help identify the different forms of Cu present in the sample: Cu(II), Cu(I), and Cu°. The Cu $2p_{3/2}$ XPS signal from samples analyzed using Al Kα X-rays is shown in Fig. 7a and the Cu O1s XPS signal is shown in Fig. 7b. The samples corresponding to these spectra were prepared by electron beam evaporation followed by either an ECR oxidization or an exposure to a humid air environment. The spectra shown as light gray circles are from a sample oxidized in the ECR O_2 plasma for 30 min. at 75°C to form a 32 nm thick oxide layer. The spectra shown as a dashed line are from a sample oxidized in the

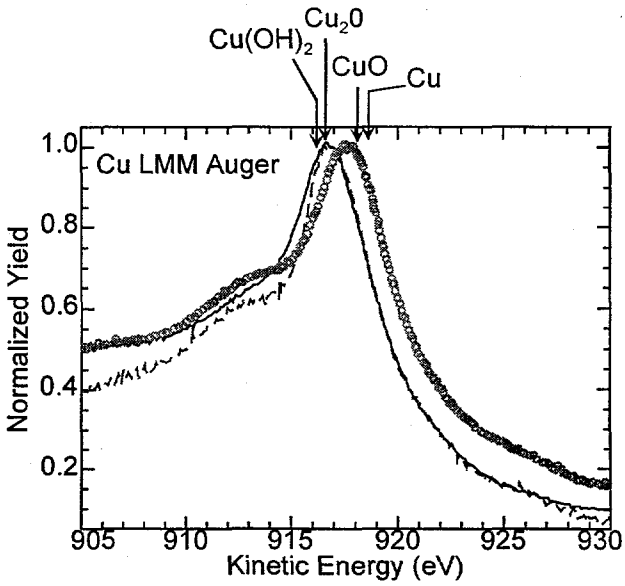

Fig. 8. A comparison of air oxidized Cu and ECR-oxidized Cu LMM auger peaks excited using Al K X-rays.

ECR O_2 plasma for 2 min. at 75°C to form a ~4 nm thick oxide layer, and the spectra shown as a solid line are from a sample exposed to a humid air environment (65% RH) for 4 days at 50°C to form ~1.5 nm thick air oxide. The Cu $2p_{3/2}$ and O 1s spectra alone are not sufficient to identify Cu vs. Cu_2O vs. CuO. The Cu LMM Auger signal is also required to identify the nature of these samples, and fig. 8 gives the Cu LMM Auger signal collected using Al Kα x-ray excitation..

The shakeup peaks demonstrated that each oxidized sample contained CuO and Cu_2O, but the ratio of CuO to Cu_2O varied. Air-oxidized sample contained a greater proportion of Cu_2O than thick ECR-grown oxides, and a thin ECR oxide sample is a good intermediate mixture of Cu_2O and CuO. The plasma treated Cu-oxides provide good test samples for comparison to air Cu-oxides. The air oxide was approximately 1.5 nm thick and predominantly Cu_2O with possibly a small amount of CuO in agreement with other work on air-formed oxides. An ion beam analysis composition-depth profile shown in fig. 9 and XPS analysis of a thick ECR-grown oxide showed that an ECR oxidized Cu sample was fully oxidized to CuO at the surface but contained a graded composition from Cu_2O to pure Cu at depth in the sample. The thickness of the CuO layer is controlled by masking the sample to control the sample exposure time to the plasma. Note, an additional peak appeared in the O 1s spectra for ECR oxidized samples, but this peak has not yet been identified.

The unirradiated ECR-oxidized samples have a significant quantity of CuO at the surface. Thermodynamically, this CuO is more stable to sulfidization than Cu_2O and can form a good passivating layer. Possible thermodynamic reactions and their associated free energies are given in Table I. However, if the CuO is "broken" such as through ion-irradiation creating defects for rapid transport of Cu to the surface, then the sulfidation reaction can occur. Air-oxidized Cu already has a sufficient quantity of Cu_2O at the surface which will sulfidize without the need for additional defects.

Ion irradiation not only increases the number of vacancies but it and can also cause a reduction in the Cu oxidation state. A CuO/Cu sample formed by ECR oxidation which was then irradiated with 200 keV Cu^+ to a fluence of $2x10^{15}$ Cu/cm^2 demonstrated (not shown) that the Cu(II) shakeup peak is reduced suggesting that CuO is reduced to Cu_2O or Cu. However, this does not discern between reduction as a result of increased defect concentration or a change in composition. The thermodynamics of the possible reaction pathways suggests that by reducing CuO to Cu_2O (or Cu) permits the sulfidation reaction to proceed which is more thermodynamically favorable than sulfidation of CuO. Still this tells us nothing about the kinetics of the reaction and the fact that a greater amount of sulfide formation occurs for the higher fluence irradiation may suggest that greater solid-state transport occurs for the higher fluence irradiation. By decreasing the fluence level and changing the ion species we will be able to determine if the reduction of CuO occurs

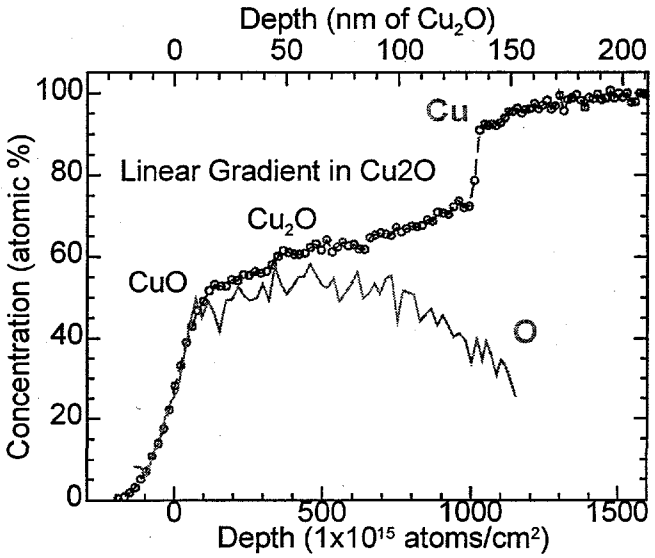

Fig. 9. Composition-depth profile determined using RBS analysis of an ECR oxidized Cu sample exposed to the plasma for 49 min. at 150°C in order to form a thick oxide layer. The surface layer is CuO and turns into a Cu_2O layer with a composition gradient at depth in the sample. The sample was analyzed using a 2.8 MeV He^+ ion beam with 164° scattering angle.

primarily as a result of atomic collisions or through deposition of energy into electron ionization.

TABLE I

Reaction	ΔG (kcal/mole)
$Cu (s) + 1/2\ O_2 (g) = CuO (s)$	-30.4
$2\ Cu (s) + 1/2\ O_2 (g) = Cu_2O (s)$	-35.0
$Cu_2O (s) + 1/2\ O_2 (g) = 2\ CuO (s)$	-25.8
$2\ Cu (s) + H_2S (aq) + 1/2\ O_2 (g) = Cu_2S (s) + H_2O (l)$	-70.8
$Cu_2O (s) + H_2S (aq) = Cu_2S (s) + H_2O (l)$	-35.8
$2\ CuO (s) + H_2S (aq) = Cu_2S (s) + H_2 (g) + O_2 (g)$	+46.7
$2\ CuO (s) + H_2S (aq) = Cu_2S (s) + H_2O (l) + 1/2\ O_2 (g)$	-10

SUMMARY CONCLUSIONS

1. ECR plasma-oxidized Cu, plus ion irradiation yields good test structures for determining the controlling mechanisms of Cu sulfidation by H_2S in humid air environments. The ECR oxidation produces a CuO surface layer on top of a layer with graded composition from Cu_2O to Cu. Furthermore, even air oxides show small quantities of CuO, but the thin oxide layer is primarily Cu_2O.

2. The type of Cu-oxide (CuO vs. Cu_2O) and defect level in the oxide are more important for controlling the sulfidation reaction than oxide thickness. An undamaged CuO surface prevents H_2S sulfidation at 24°C.

3. The critical ion implantation fluence was determined which created sufficient point defect to allow solid-state diffusion to proceed and allowed sulfidation of a CuO/Cu sample. The critical fluence was $>1x10^{12}$ Cu/cm^2 when irradiated with 200 keV Cu^+ which produced ~0.002 vacancies/atom in Cu_2O, calculated using a TRIM computer code. This critical vacancy level would be less in CuO.

4. This work suggests possible rate controlling sulfidation reaction mechanisms: Cu & Cu^+ will sulfidize but Cu^{++} will not sulfidize. Therefore, either defects in CuO enable Cu diffusion through CuO to drive the reaction, or irradiation reduces the oxidation state of Cu^{++} in CuO to allow sulfidation. That is, either O is "snow-plowed" in front of sulfidation front or O becomes buried due to Cu out-diffusion.

ACKNOWLEDGEMENTS

The authors are indebted to Ken Minor and Sam Lucero for their invaluable technical support. Sandia is a multiprogram laboratory operated by Sandia Corporation, a Lockheed Martin Company, for the United States Department of Energy under Contract DE-AC04-94AL85000. Specifically, the authors were funded by Sandia Laboratory Research Foundations, a Laboratory Directed Research and Development Program, and the US DOE Office of Basic Energy Sciences.

REFERENCES

1. D. A. Jones, Principles and Prevention of Corrosion, Prentice Hall, Englewood Cliffs, NJ, p. 198 (1992)
2. M. Pourbaix, Atlas of Electrochemical Equilibria in Aqueous Solutions, NACE, Houston (1974)
3. M. F. Ashby, Third International Conference on Strength of Metals and Alloys, vol. 2, Cambridge, England, p. 8 (1973)

4. M. F. Ashby, Acta Met. **20**, 887 (1972).
5. F. W. Crossman and M. F. Ashby, Acta Met. **23**, 425 (1975)
6. J. P. Franey, T. E. Graedel, and G. W. Kammlott, Atmospheric Corrosion, ed. By W. H. Ailor, John Wiley and Sons, New York, p. 383 (1982)
7. T. E. Graedel, J. P. Franey, and G. W. Kammlott, Corrosion Science **23**, 1141 (1983)
8. T. E. Graedel, J. P. Franey, G. J. Gualtieri, G. W. Kammlott, and D. L. Malm, Corrosion Science **25**, 1163 (1985)
9. T. E. Graedel, J. P. Franey, G. W. Kammlott, J. M. Vandenberg, and P.L. Key, J. Electrochem. Soc. **134**, 1632 (1987)
10. R.E. Lobnig and C.A. Jankoski, J. Electrochem. Soc. **145**, 946 (1998).
11. S. P. Sharma, J. Vac. Sci. Technol. **16**, 1557 (1979)
12. P. B. P. Phipps and D. W. Rice, in Corrosion Chemistry, G. R. Brubaker and P. B. P. Phipps, Ed., ACS Symp. Ser. 89. Am. Chem. Soc., p. 256-258 (1979)
13. P. W. Brown and L. W. Masters, in Atmospheric Corrosion, W. H. Ailor, Ed., Electrochemical Society, p. 31 (1982)
14. T. E. Graedel, Corrosion Science **38**, 2153 (1996)
15. J. Tidblad and T. E. Graedel, Corrosion Science **38**, 2201 (1996)
16. "Primer on Molecular Genetics", revised by Denise Casey, Human Genome Management Information System, Oak Ridge National Laboratory (1992).
17. See for example: "High Throughput Microchannel DNA Sequencer" by Joe W. Balch, http://www-bio.llnl.gov/bbrp/html/balch.ab.html; and "High Density Gridded Array Production Using a Second Generation Spotting System" by A. Copeland, J. Pesavento, R. Mariella, and D. Masquelier, http://www.llnl.gov/automation-robotics/poster.1.html
18. See for example: V.E. Velculescu, L. Zhang, B. Vogelstein, and K.W. Kinzler, Science **270**, 484 (1995); or L. Zhang, W. Zhou, V.E. Velculescu, S.E. Kern, R.H. Hruban, S.R. Hamilton, B. Vogelstein, and K.W. Kinzler, Science **276**, 1268 (1997).
19. R.F. Service, Science **283**, 165 (1999).
20. S.B. Zhang, S.H. Wei, A. Zunger, and H. Katayamayoshida, Phys. Rev. B **57**, 9642 (1998); see also R. W. Cahn, Nature **389**, 121 (1997).
21. M. Scorocco, Chem. Phys. Lett. **63**, 52 (1979).
22. S. Poulson, P.M. Parlett, P. Stone, and M. Bowker, Surface and Interface Analysis **24**, 811 (1996).
23. S.K. Chawla, B.I. Rickett, N. Sankarraman, and J.H. Payer, Corrosion Science **33**, 1617 (1992).
24. C. R. Clayton, G. P. Halada, and S. V. Kagwade, Electrochemical Society Proceedings, 98-17, p. 223 (1999).
25. N. E. Cipollini, J. Electrochem. Soc. **129**, 1517 (1982).
26. M.P. Siegal, J.C. Barbour, P.N. Provencio, D.R. Tallant, and T.A. Friedmann, Appl. Phys. Lett. **73**, 759 (1998).
27. W. G. Breiland and K. P. Killeen, J. Appl. Phys. **78,** 6726 (1995)
28. B. J. Mulder, Phys. Stat. Sol. (a) **13,** 79 (1972).
29. S. M. Butorin et al., Phys. Rev. Lett. **77**, 574 (1996)
30. P. Glans et al., Phys. Rev. Lett. **76**, 2448 (1996)
31. N.M. Markovic, H.A. Gasteiger and P.N. Ross, J. Phys. Chem. **99**, 3411 (1995).
32. K. Pasztor, A. Sekiguchi, N. Shimo, N. Kitamura and H. Masuhara, Sensors and Actuators B **12**, 225 (1993).
33. M. Kupper and J.W. Schultze, J. Electroanal. Chem. **427**, 129 (1997).
34. J.A. Shatkin, H. Szejnwald Brown and S. Licht, Anal. Chem. **67**, 1147 (1995).
35. Y. S. Chu, I. K. Robinson, A. A Gewirth, J. Chem. Phys. in press.
36. M. F. Toney, A. J. Davenport, L. J. Oblonsky, M. P. Ryan and C. M. Vitus, Phys. Rev. Lett. **79**, 4282(1997).